# Molecular-beam mass-spectrometric study of the flame structure of composite propellants based on nitramines and glycidyl azide polymer at a pressure of 1 MPa

**4 AUTHORS**, INCLUDING:

Alexander A Paletsky
Russian Academy of Sciences
**39** PUBLICATIONS **197** CITATIONS

SEE PROFILE

A. G. Tereshchenko
Russian Academy of Sciences
**23** PUBLICATIONS **111** CITATIONS

SEE PROFILE

# Molecular-Beam Mass-Spectrometric Study of the Flame Structure of Composite Propellants Based on Nitramines and Glycidyl Azide Polymer at a Pressure of 1 MPa

**E. N. Volkov,**[1] **A. A. Paletsky,**[1] **A. G. Tereshchenko,**[1] **and O. P. Korobeinichev**[1]

**A study was performed of the chemical and thermal structure of flames of model composite propellants based on cyclic nitramines (RDX and HMX) and an active binder (glycidyl azide polymer) at a pressure of 1 MPa. Propellant burning rates were measured. The chemical structure of the flame was studied using molecular-beam mass spectrometry, which previously has not been employed at high pressures. Eleven species ($H_2$, $H_2O$, HCN, $N_2$, CO, $CH_2O$, NO, $N_2O$, $CO_2$, $NO_2$, and nitramine vapor) were identified, and their concentration profiles, including the composition near the burning surface were measured. Two chemical-reaction zones were observed. It was shown that flames of nitramine/glycidyl azide polymer propellants are dominated by the same reactions as in flames of pure nitramines.**

**Key words: flame structure, composite solid propellant, nitramines, glycidyl azide polymer, probing mass spectrometry.**

## INTRODUCTION

The combustion mechanism of energetic materials is of considerable interest from both a fundamental and a practical point of view. Knowledge of the real physicochemical processes involved in the combustion of condensed systems is required to solve the fundamental research problem consisting of developing a model for the combustion of condensed systems based on detailed kinetic mechanisms. The current status of computational means and techniques allows the modeling of the combustion of energetic materials at the molecular level, but this requires knowledge of the combustion chemistry of these materials. Flame structure studies are the main source of information on the mechanism and kinetics of the chemical reactions involved in the combustion of energetic materials. An analysis of flame structure data for condensed systems provides information on the composition of the products formed by condensed-phase reactions. This, in turn, provides an understanding of what reactions proceed in the condensed phases and what their mechanism is. In addition, the product composition near the burning surface of energetic materials is the boundary condition in combustion modeling. The chemical structure of flames of energetic materials also gives information on the mechanism and kinetics of the subsequent chemical transformations of gasification products responsible for heat release in the gas phase. Information on both condensed- and gas-phase reactions is required to develop a model for the combustion of energetic materials. Without such information, it is impossible to develop a valid combustion model that would predict the burning rate and other ballistic characteristics of energetic materials.

Propellant based on cyclic nitramines (RDX and HMX) and azide polymers [such, as glycidyl azide polymer (GAP), 3,3′-bisazidomethyloxetane polymer (BAMO), and 3-azidomethyl-3-methyloxetane polymer (AMMO)] are characterized by a fairly high specific im-

[1]Institute of Chemical Kinetics and Combustion, Siberian Division, Russian Academy of Sciences, Novosibirsk 630090; korobein@ns.kinetics.nsc.ru.

pulse while generating little smoke. Their research is therefore of considerable interest. In the literature there are many papers on the combustion of nitramine/GAP propellants. Data on the thermal structure of the combustion wave of HMX/GAP and RDX/GAP propellants were published in [1–3] and [1, 2], respectively. The chemical structure of flames for laser-assisted combustion of nitramine/azide polymer propellants has been studied [4] using mass-spectrometric microprobe sampling at atmospheric pressure. RDX/BAMO, RDX/GAP, and HMX/GAP propellants have been studied. Generalizing the results obtained, Litzinger et al. [4] came to the conclusion that the laser-assisted combustion of nitramine/azide polymer propellants is dominated by the chemical reactions characteristic of nitramines. Azide polymers also affected the flame structure, for example, the length of the first reaction zone and the location of the beginning of the second reaction zone. However, the findings differed for the three propellants studied. Therefore, it was concluded [4] that a detailed numerical modeling of the combustion of these propellants is required to understand and explain the observed regularities. Combustion models for HMX/GAP and RDX/GAP propellants are presented in [5, 6]. Generally, there is reasonable agreement between calculated [5] and experimental [4] flame structures of HMX/GAP at atmospheric pressure under laser radiation. For the RDX/GAP based propellant, the results of calculations [6] and experiments [4] are in much worse agreement. This is partly due to the fact that the calculation of the element balance using experimental flame species concentration profiles results in a worse fit than that for the HMX/GAP propellant [4]. Thus, the combustion models for nitramine/GAP propellants presented in [5, 6] cannot predict the combustion characteristics with necessary accuracy. Puduppakkam and Beckstead [7] proposed an alternative model for RDX/GAP propellant combustion that adequately describes the experimental temperature profile obtained in [4] for laser-assisted combustion ($100 \ \mathrm{W/cm^2}$) at atmospheric pressure. Puduppakkam and Beckstead [7] do not give the chemical flame structure calculated for these conditions but they argue that it agrees with experimental findings. It should be noted that in [4] nitramine vapor was not detected in flames of nitramine/azide polymer propellants, which may be attributed to their decomposition or deposition on the inner walls of the microprobe, whereas the combustion models of [5–7] predict the existence of nitramine vapor near the propellant burning surface.

Previously [8, 9], using probing molecular-beam mass spectrometry, we studied the HMX/GAP flame

structure in the case of self-sustaining combustion at a pressure of 0.5 MPa. A careful analysis of the near-surface flame zone and calibrations showed that HMX vapor was present in a narrow zone $\approx 100 \ \mu\mathrm{m}$ wide near the HMX/GAP burning surface. Further validation and improvement of the combustion models for HMX/GAP and RDX/GAP propellants requires a considerable body of experimental data (especially on the flame structure). In the work described here, we studied the self-sustaining combustion of uncured HMX/GAP and RDX/GAP composite propellants at a pressure of 1 MPa. Emphasis was on the thermal and chemical structure of these propellant flames. Special attention was given to an analysis of the narrow near-surface combustion zone to determine the product composition and establish the presence of nitramine vapor in this zone.

## EXPERIMENTAL TECHNIQUE

The GAP used in the present work was synthesized and certificated at St. Petersburg Technological University. GAP is a yellow viscous liquid. Its main characteristics are as follows:

structural formula

$$C_2H_5\!-\!C\!\equiv\![CH_2(-\!O\!-\!CH_2\!-\!CH(CH_2\!-\!N_3)\!-\!)_n OH]_3;$$
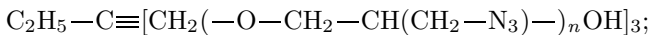
elemental composition $C_{60}H_{104}N_{54}O_{21}$;
mean molecular mass 1976;
density $1.275 \ \mathrm{g/cm^3}$;
enthalpy of formation 611 kJ/kg.

The main characteristics of HMX and RDX are listed in Table 1.

The propellant samples were prepared by mixing a crystalline nitramine powder (a mass fraction of 80%) and GAP (20%). The nitramine powder consisted of particles of two fractions (150–250 $\mu$m and $\leqslant 20 \ \mu$m) taken in a mass proportion of 1 : 1. The mixture was prepared in dry air. In the final form, it was a viscous plastic mass. Before use, the mixture was placed in a glass flask, which was then evacuated to a pressure of $10^{-1}$–$10^{-2}$ torr. Propellant samples of diameter 6 mm were used. The density of the HMX/GAP samples was $1.69 \ \mathrm{g/cm^3}$, and that of the RDX/GAP samples was $1.64 \ \mathrm{g/cm^3}$, i.e., $\approx 98\%$ of the corresponding calculated maximum density of the propellants.

The burning rate of the composite propellants was measured by video records of the process with a measurement accuracy of $\pm 5\%$.

TABLE 1

Main Characteristics of HMX and RDX

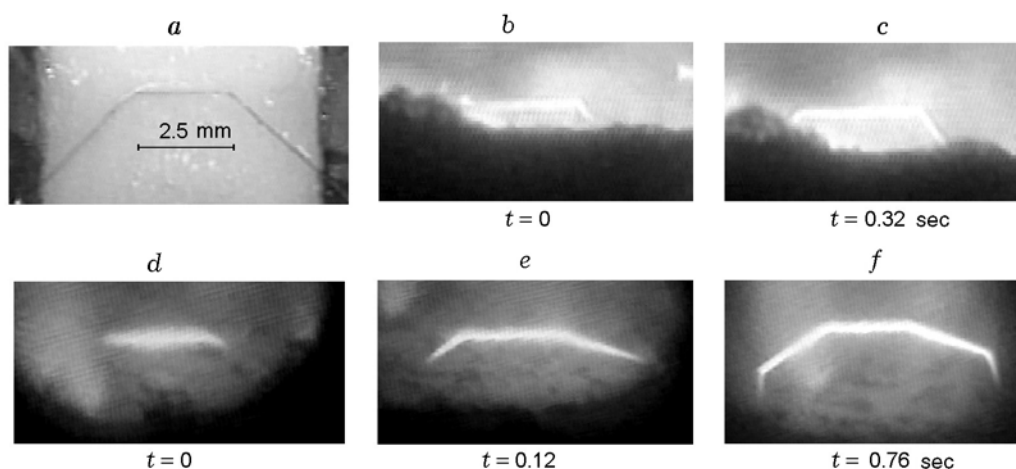| Characteristics | HMX ($C_4H_8N_8O_8$) | RDX ($C_3H_6N_6O_6$) |
|---|---|---|
| Molecular weight, g/mole | 296 | 222 |
| Density, $g/cm^3$ | 1.9 | 1.81 |
| Enthalpy of formation, kJ/kg | 297.0 | 320.6 |
| Oxygen balance, $O_2/CO_2$, $H_2O$, % | $-21.6$ | $-21.6$ |



**Fig. 1.** Video images of the exit of a thermocouple embedded in a HMX/GAP sample into the gas phase at a pressure of 1 MPa: arrangement of the thermocouple in the sample (a), transmitted-light observation parallel to the burning surface (b and c), and reflected-light observation at an angle of $30°$ to the burning surface (d–f).

Flame temperature profiles were measured with WRe(5%)–WRe(20%) ribbon thermocouples (13–15 $\mu$m thick and $\approx$140–150 $\mu$m wide), which were embedded into the samples using a special technology. The thermocouples were U-shaped with a leg $\approx$2.5–3.0 mm long (Fig. 1). The samples were placed in cylinders made of tissue paper which was previously impregnated with an ammonium perchlorate solution and dried. Samples of diameter $\approx$6–8 mm with the thermocouple embedded in them were burned in a constant-pressure bomb. The exit of the thermocouple from the burning sample (see Fig. 1) was video recorded, and the video records were used to determine the correctness of the temperature profile measurements. The profile was taken into consideration only if at the time of exit of the thermocouple to the gas phase, its legs were parallel to the burning surface and no particles were observed on the thermocouple surface.

The flame structure of the HMX/GAP and RDX/GAP propellants at a pressure of 1 MPa was studied on an automated mass-spectrometric complex with a molecular-beam sampling system. Combustion products were sampled from the flame using quartz (sonic) probes (opening angle of the inner cone of the probe $\approx$40$°$). Probing mass spectrometry is one of the most effective and universal experimental techniques for studying the chemical structure of solid propellant flames. However, the use of this technique for sampling combustion products from flames inevitably leads to flame perturbations, which must be minimized. In each particular case, it is necessary to validate the technique and the data obtained. One criterion for the smallness of flame perturbations induced by the probe is similarity of concentration profiles obtained with the probe and temperature profiles measured with the thermocouple technique without the probe. The applicability of mass-spectrometric sampling at high pressures was validated earlier [8, 9] for the combustion of HMX/GAP propellants at a pressure of 0.5 MPa. As the pressure increases from 0.5 to 1 MPa, the analysis of the HMX/GAP flame structure becomes complicated. First, a pressure rise leads to a decrease in the flame width. This implies
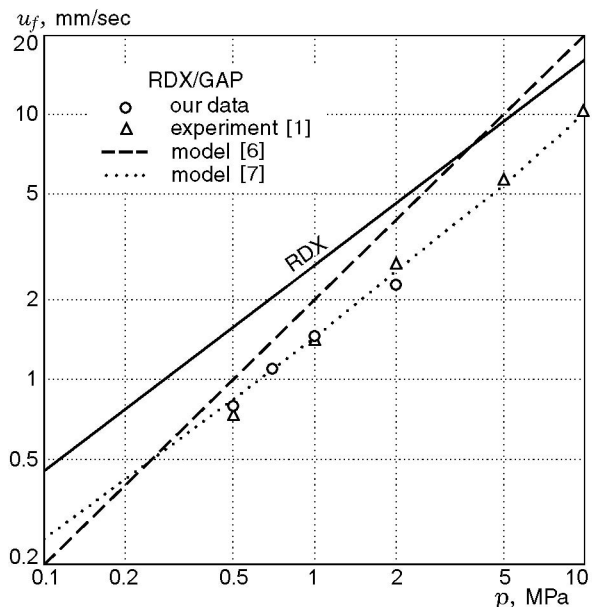
**Fig. 2.** Burning rate of RDX/GAP in comparison with the burning rate of pure RDX.



**Fig. 3.** Burning rate of HMX/GAP in comparison with the burning rate of pure HMX.

that at a pressure of 1 MPa, probes with smaller wall thickness are needed to prevent the distortion of the flame structure due to the thermal perturbation by the probe. Therefore, probes with a wall thickness near the orifice of 0.15 mm were used. In the present work, we used three identical probes since after 3 or 4 experiments, the probe became unfit because of the fusion or plugging of the inlet orifice. Second, as the pressure rises from 0.5 to 1 MPa, the burning rate increases (for HMX/GAP, from 0.96 to $\approx 1.6$ mm/sec), resulting in a decrease in the flame probing time.

## RESULTS AND DISCUSSION

### Burning Rate

RDX and HMX are monopropellants with a small negative oxygen balance and high adiabatic flame temperatures in excess of 3000 K. Nevertheless, the burning rates of RDX and HMX are not very high, and they are characterized by a fairly high pressure exponent ($\approx 0.8$). The negative oxygen balance implies that the oxygen available in RDX and HMX molecules is not enough to oxidize the entire carbon and hydrogen to $CO_2$ and $H_2O$, respectively. The addition of a polymer binder to RDX or HMX with the aim of producing propellants leads to an even greater deficit of oxygen. This causes a decrease in the temperature of the final combustion products and, as a consequence, a decrease in heat feed-
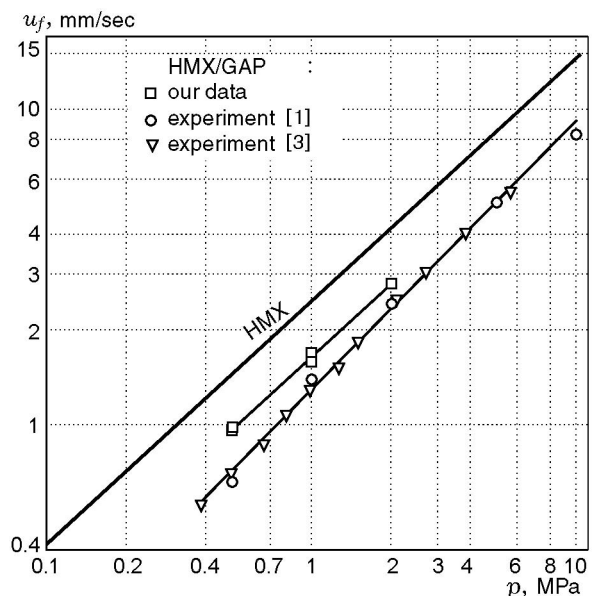
back from the gas phase to the condensed phase, which is manifested as slowing down of the combustion. Figure 2 compares the burning rates of an RDX based propellant with 20% GAP with the burning rate of pure RDX. It is evident that the burning rate of the propellant is lower than that of pure RDX. A comparison of our data on the burning rate of RDX/GAP with the data of [1] shows that they are in good agreement. The model of [7] adequately describes the burning rate of 80/20 RDX/GAP, whereas the model of [6] gives overestimated values. The burning rate of 80/20 HMX/GAP was measured in [1, 3], and the results obtained in these studies are close to each other (Fig. 3). In the present study, the HMX/GAP burning rate was measured at pressures of 0.5–2.0 MPa. The propellant studied here has a slightly higher burning rate but, generally, the obtained pressure dependence of the burning rate is close to the data of [1, 3].

### Thermal Flame Structure

Figure 4 gives the primary and averaged temperature profiles for HMX/GAP and RDX/GAP propellants. It is evident that the primary profiles are characterized by a small spread due to the heterogeneity of the burning surface, which is related primarily to the presence of undecomposed GAP on it. On the burning surface of HMX/GAP at a pressure of 1 MPa, as well as at 0.5 MPa [9], undecomposed GAP was observed as dark
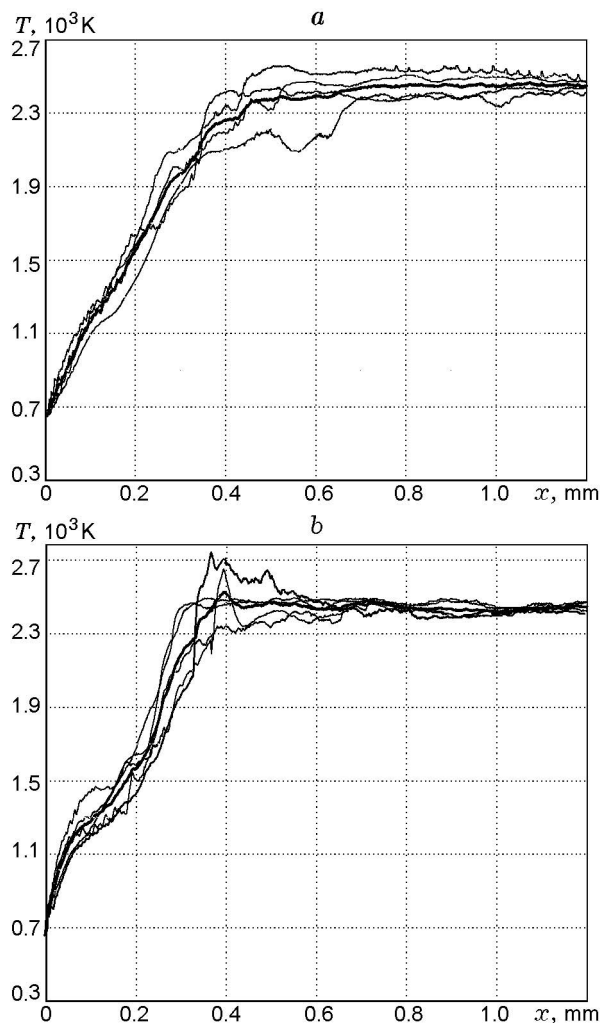
**Fig. 4.** Primary (thin curves) and averaged (thick curves) temperature profiles in HMX/GAP (a) and RDX/GAP (b) flames at a pressure of 1 MPa (without the radiation correction).



**Fig. 5.** Flame temperature profiles for nitramine/GAP propellants at a pressure of 1 MPa (with the radiation correction).

particles but in a much smaller amount. On the burning surface of RDX/GAP at a pressure of 1 MPa, small carbon formations (particle aggregates) rather than individual particles were observed. The larger amount of the carbon residue on the RDX/GAP burning surface indicates that the fraction of condensed-phase decomposition of GAP is smaller than that in the case of HMX/GAP. Two of the five primary temperature profiles for RDX/GAP are characterized by the presence of a segment with a temperature exceeding the final flame temperature (Fig. 4b). This is likely related to a reduction in the local fuel-to-oxidizer ratio and, hence, to approach to the stoichiometry.

The averaged temperature profiles were corrected for the heat losses by the thermocouple due to radiation (radiation corre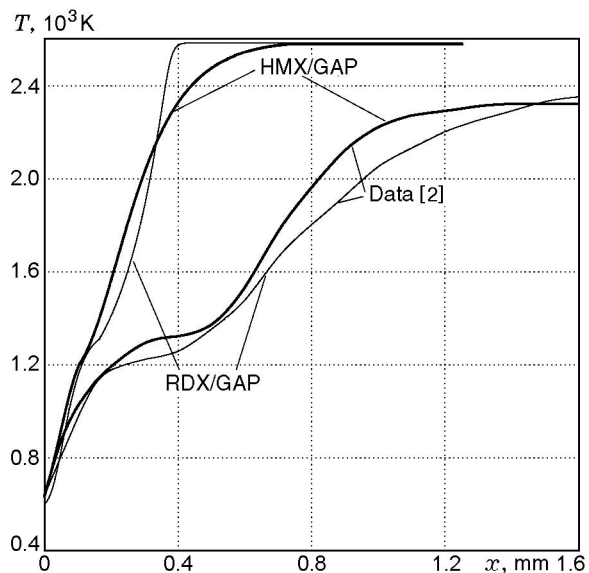ction) and then smoothed out. Figure 5 gives averaged and smoothed profiles for HMX/GAP and RDX/GAP propellants at a pressure of 1 MPa. For both propellants, the averaged final flame temperature is ≈2580 K. However, the distances at which this value is reached are different: 0.7 mm for HMX/GAP and 0.4 mm for RDX/GAP. Thermodynamic calculations using the ASTRA code [10] showed that at a pressure of 1 MPa, the adiabatic combustion temperature for HMX/GAP is 2608 K, and for RDX/GAP, it is 2617 K. The small difference between the experimental and calculated values of the final temperature is within the error of the thermocouple technique.

A comparison of the temperature profiles with the data of [2] (see Fig. 5) shows that there are two main differences between them. The first is the presence of a long plateau (at a temperature of ≈1200–1300 K) on the profiles obtained in [2]. The second difference concerns the temperature of the final products: according to our measurements, it is ≈2580 K for both propellants, whereas in [2], it reaches only 2320 and 2360 K for HMX/GAP and RDX/GAP propellants, respectively. Before the appearance of [11], we believed that the most probable reason of that significant difference is the difference between the characteristics of the examined propellant samples, namely, the densities of the propellants and the properties of the GAP used. For example, the density of the HMX/GAP propellant used in [1, 2] was only 88% of the maximum calculated density of the propellant, whereas in our case, it reaches ≈98%. The understanding of the reasons of such significant differences

in the temperature profiles is hindered because in [1, 2], there is no information on the procedure of preparing the propellants, the method of calculating the adiabatic temperature, and the parameters used in the thermodynamic calculations (in particular, the enthalpy of formation of GAP). The appearance of a paper [11] has made it even more difficult to perform a correct comparison of our data with the results of [1, 2, 11]. The characteristics of the HMX/GAP propellant (element composition, density, and adiabatic temperature) presented in [11] differ considerably from those presented in [1, 2]. The element composition of the propellant was revised. The density of the propellant increased from 1.52 to 1.74 $g/cm^3$, and the adiabatic temperature of the propellant decreased from 2776 to 2693 K. At the same time, the parameters describing the temperature profiles (burning-surface temperature, temperature gradient near the burning surface, final flame temperature, etc.) remained the same. No explanations is given in [11].

### Chemical Flame Structure

Mass-spectrometric analysis of gas samples taken from flames of the nitramine/GAPs identified the following species: $H_2$ (2), $H_2O$ (18 and 17), HCN (27, 26, and 14), CO (28 and 12), $N_2$ (28 and 14), $CH_2O$ (29 and 30), NO (30 and 14), $CO_2$ (44, 28, and 22), $N_2O$ (44, 30, 28, and 14), $NO_2$ (46, 30, and 14), and nitramine vapor (75, 46, 42, 30, and 29). The mass peaks used to identify these species and determine their concentrations are given in parentheses. The contributions from species having identical mass peaks were separated using mass spectra of individual species obtained in calibration experiments. The concentrations of the identified species were determined with the use of the calibration coefficients measured in calibration experiments. For most gases, the accuracy of the calibration coefficients is $\pm 5\%$, and for $H_2O$, HCN, and $NO_2$, it is $\pm 10\%$. Obtaining HMX vapor ($HMX_{vap}$) and RDX vapor ($RDX_{vap}$) at atmospheric pressure and determining their calibration coefficients is a very difficult challenge. The procedure used to determine the calibration coefficient of HMX vapor is described in [8, 9]. The calibration coefficient of RDX vapor was determined by the same procedure. The accuracy of the calibration coefficient for HMX and RDX vapor is $\pm 15\%$. The values of these calibration coefficients are very important for a correct determination of the composition near the burning surface of nitramine propellants. Therefore, in the future, we are planning to perform additional calibration experiments to check these values.
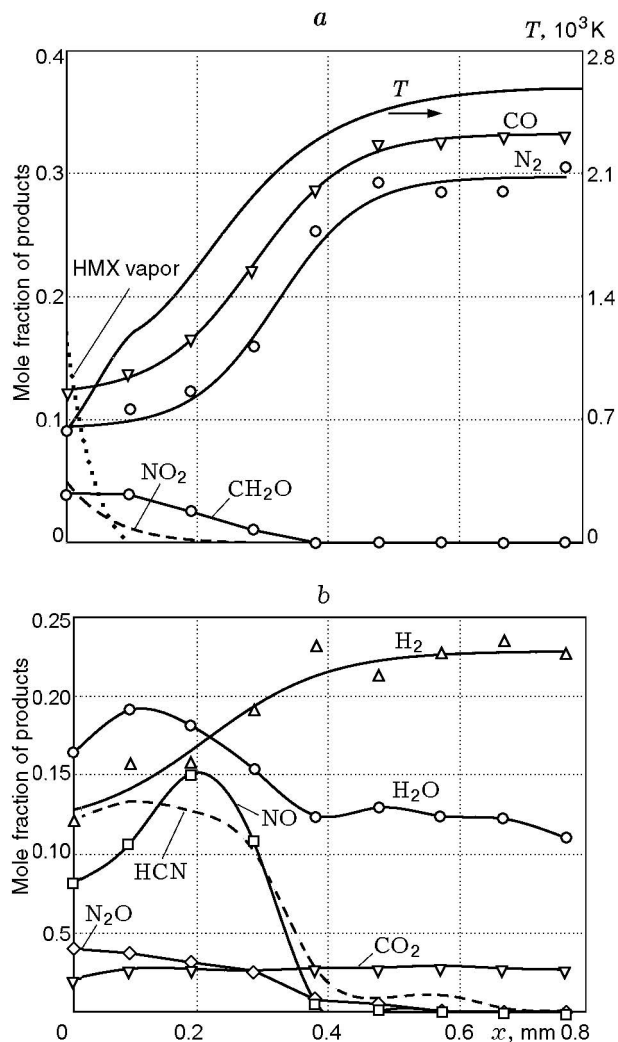


**Fig. 6.** HMX/GAP flame structure at a pressure of 1 MPa.

The location of the burning surface on the concentration profiles was determined by the moment the probe came in contact with the liquid layer on the propellant burning surface. This moment is characterized by a sudden change in the intensities of most of the mass peaks, which obviously corresponds to a density change of the sampled products in the gas to condensed phase transition. The moment of contact of the probe with the burning surface was determined by video recording, which was synchronized with mass-spectrometric measurements.

The product compositions (in mole fractions) near the burning surfaces of HMX/GAP and RDX/GAP at a pressure of 1 MPa, obtained with a thick-walled quartz probe with a wall thickness of $\approx 0.5$ mm and an orifice

TABLE 2

Composition (in Mole Fractions) of Products near Burning Surface
of HMX/GAP and RDX/GAP Propellants at a Pressure of 1 MPa

| $T_s$, K | $H_2$ | $H_2O$ | HCN | $N_2$ | CO | NO | $CH_2O$ | $CO_2$ | $NO_2$ | $N_2O$ | $HMX_{vap}$ | $RDX_{vap}$ |
|---|---|---|---|---|---|---|---|---|---|---|---|---|
| HMX/GAP | | | | | | | | | | | | |
| 638* | 0.12 | 0.16 | 0.12 | 0.09 | 0.12 | 0.08 | 0.04 | 0.02 | 0.05 | 0.04 | 0.17 | — |
| RDX/GAP | | | | | | | | | | | | |
| 635 | 0.12 | 0.11 | 0.10 | 0.01 | 0.11 | 0.04 | 0.02 | 0 | 0.09 | 0.06 | — | 0.33 |

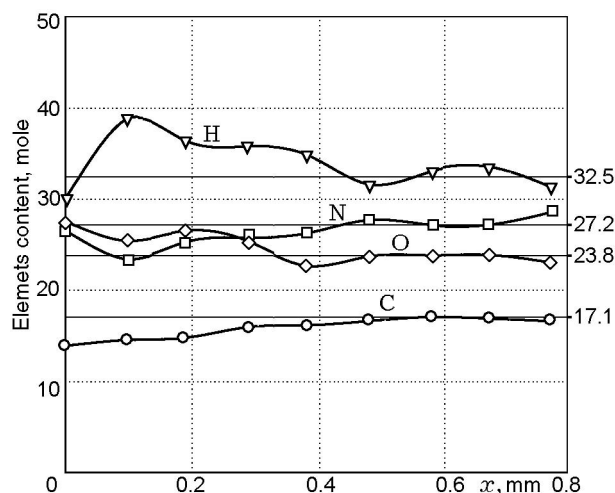**Note.** The data of [1] are marked by an asterisk.



**Fig. 7.** Element distribution in the HMX/GAP flame at a pressure of 1 MPa.

diameter of 10–25 $\mu$m, are given in Table 2. Products such as $N_2$, CO, $CO_2$, $CH_2O$, $H_2O$, HCN, and $H_2$ can be formed from both nitramines [12] and GAP [13]. Nitrogen oxides ($NO_2$, NO, and $N_2O$) and nitramine vapor are formed only from nitramines. The mass fraction of HMX (RDX) vapor in the identified products near the propellant burning surface was $\approx$70% ($\approx$80%). The question of what fraction of nitramine is decomposed in the condensed phase, and what fraction of it vaporizes is very important for an understanding of the combustion chemistry of nitramines and nitramine based propellants. For combustion of pure nitramine, knowledge of the product composition near the burning surface (in the gas phase) and accounting for diffusion provide an answer to this question. For the propellant combustion, accounting for the mass fraction of nitramine in the propellant is needed since the decomposition of GAP also yields gaseous products. The presence of incompletely decomposed GAP on the burning surface makes it impossible to determine the quantitative ra-

tio between the vaporized and decomposed nitramine. Nevertheless, taking into account that in the starting propellant, the mass fraction of nitramine is 80%, it is possible to draw a qualitative conclusion that in the propellant combustion, most of the starting nitramine is transferred to the gas phase as vapor.

At the HMX/GAP propellant surface at a pressure of 1 MPa, as well as at 0.5 MPa, mass peaks 39, 41, 42, and 43 were detected, which have not yet been identified (except for part of peak 42, which is assigned to HMX vapor). These peaks are most likely associated with the combustion/decomposition products of GAP. Like in the flame at a pressure of 0.5 MPa, their intensities decreased with distance from the burning surface. In the case of the RDX/GAP propellant at a pressure of 1 MPa, such peaks were not detected, which is apparently explained by the lower degree of condensed-phase decomposition of GAP.

The nitramine/GAP flame structure at a pressure of 1 MPa was studied using a thin-walled quartz probe with an orifice diameter of 15 $\mu$m and a wall thickness near the orifice of $\approx$0.15 mm. A comparison of the concentration profiles obtained with the thick-walled and thin-walled probes for nitramine/GAP propellants at a pressure of 1 MPa shows that they coincide with good accuracy at a distance of $\approx$0.2 mm from the burning surface. For most of the products, the deviation from the average concentration values at this distance is within $\pm$10%. The thick-walled probe introduces smaller perturbations into the combustion product composition near the burning surface; therefore, the propellant flame structure at a pressure of 1 MPa obtained with the thin-walled probe was supplemented at two points (on the burning surface and in the next after it) by the combustion product compositions obtained with the thick-walled probe.

The HMX/GAP flame structure at a pressure of 1 MPa and the element content profiles in the flame are presented in Figs. 6 and 7. At a pressure of 1 MPa, as well as at 0.5 MPa [9], two zones of chemical reac-
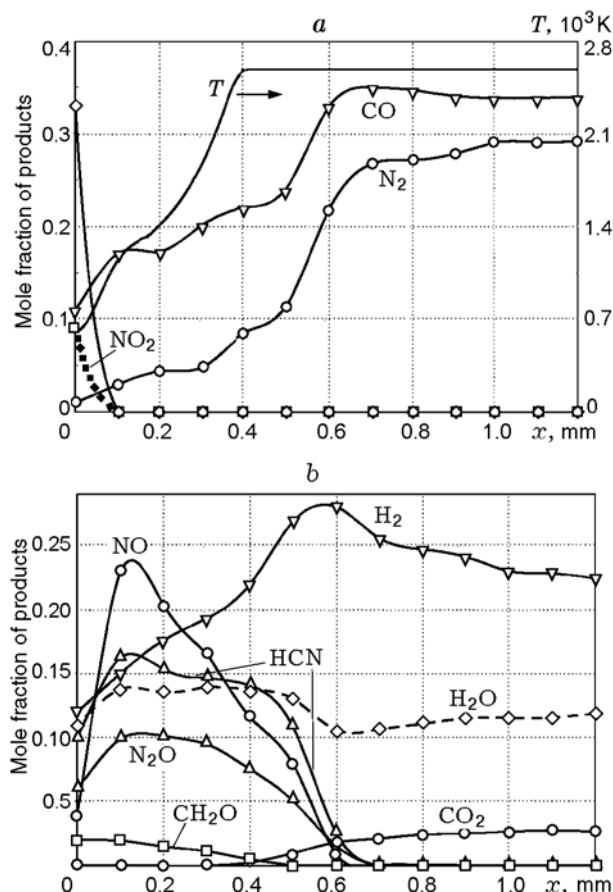
**Fig. 8.** RDX/GAP flame structure at a pressure of 1 MPa.



**Fig. 9.** Element distribution in the RDX/GAP flame at a pressure of 1 MPa.

tions were found: a zone of consumption of HMX vapor and $NO_2$ with the formation NO, HCN, CO, $H_2$, and $N_2$, a zone of consumption of $N_2O$, $CH_2O$, NO, and HCN with the subsequent formation of CO, $H_2$, and $N_2$. In the first zone, the temperature increases from 640 to $\approx$1200 K, and in the second zone, from $\approx$1200 to $\approx$2350 K. At a pressure of 1 MPa, as well as at 0.5 MPa, the zone of HCN consumption is wider than that for the other products. The element distributions over the flame zone (see Fig. 7) were calculated from the concentration profiles of the combustion products presented in Fig. 6 ignoring the diffusion fluxes of the products and were then normalized by 1 kg. The maximum deviation for the N and O concentrations is $\approx$15% of the initial values, and for the elements C and H, the maximum deviations are $\approx$20 and $\approx$25%, respectively.

The RDX/GAP flame structure at a pressure of 1 MPa and the element distributions in the flame are shown in Figs. 8 and 9. Generally, the product concentration profiles for the RDX/GAP and HMX/GAP flames are similar; there are only some, mostly quan-
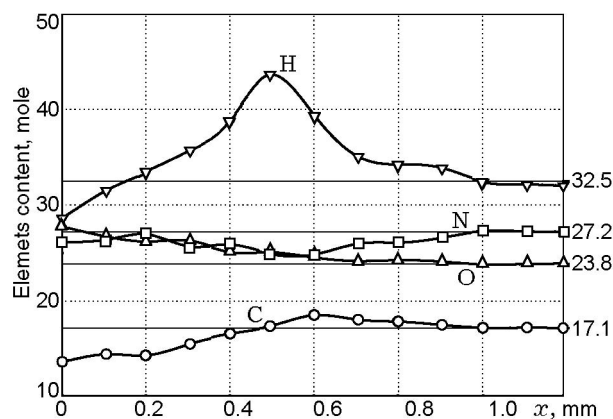
titative, differences between them. In particular, complete consumption of $CH_2O$, $N_2O$, NO, and HCN in the RDX/GAP flame occurs at a larger distance ($\approx$0.6 mm) from the burning surface than in case of the HMX/GAP propellant ($\approx$0.4 mm). In the case of the RDX/GAP propellant, the $NO_2$ and $N_2O$ concentrations are higher both near the burning surface and in the flame zone, and the $CH_2O$ concentration is lower.

In the nitramine/GAP flame at a pressure of 1 MPa, two main zones of chemical reactions are observed. In the first, low-temperature (dark) zone, the decomposition of nitramine vapor and the oxidation of formaldehyde by nitrogen dioxide occur. Most of the $NO_2$ and HMX vapor is consumed at a distance $\lesssim$0.1 mm from the burning surface with the formation of NO, CO, $H_2$, and $N_2$. In the second, high-temperature zone, the main reaction is the oxidation of hydrogen cyanide by nitric oxide to the formation of the final products CO, $N_2$, and $H_2$. In [14, 15], it was found that this reaction is the main one in the high-temperature zone of RDX [14] and HMX [15] flames. Thus, nitramine/GAP flames are dominated by the same reactions as in flames of pure nitramines. In nitramine flames, the widths of the zones of consumption of $CH_2O$ and $NO_2$ coincide, HCN is completely consumed, and NO is present in the final combustion products [14, 15]. GAP affects the flame structure of the propellants in such way that the zone of $CH_2O$ consumption becomes larger than the zone of $NO_2$ consumption and the zone of HCN consumption is larger than the zone of NO consumption. This is due to the fact that the decomposition of GAP produces additional amounts of $CH_2O$ and HCN, and the amounts of NO and $NO_2$ formed from nitramines are not sufficient to oxidize them completely.

## MAIN RESULTS AND CONCLUSIONS

HMX/GAP and the RDX/GAP propellant flames were found to contain 11 species: $H_2$, $H_2O$, HCN, $N_2$, CO, $CH_2O$, NO, $N_2O$, $CO_2$, $NO_2$, and nitramine vapor (in a zone adjacent to the burning surface). The mole fraction of nitramine vapor in the products near the burning surface was determined to be 0.33 for the RDX/GAP propellant and 0.17 for the HMX/GAP propellant. It was shown that most of the nitramine is transferred to the gas phase as vapor. The burning rates of the propellants and temperature and product concentration profiles in the combustion wave were measured. The product concentration profiles in the RDX/GAP and HMX/GAP flames are similar with only some quantitative differences. Two zones of chemical reactions were distinguished. In the first narrow flame zone of width $\approx 100$ $\mu$m (adjacent to the burning surface), nitramine vapor and $NO_2$ are consumed to form NO, HCN, CO, $H_2$, and $N_2$. In the second zone, consumption of $N_2O$, $CH_2O$, NO, and HCN and formation of the final products CO, $CO_2$, $N_2$, and $H_2$ occur. It was shown that nitramine/GAP flames are dominated by the same reactions as in flames of pure nitramines. The data obtained can be used to develop and validate a combustion model for propellants based on nitramines and GAP. In the present work, the flame structure of composite propellants at a high pressure (1 MPa) was determined for the first time using molecular-beam mass spectrometry.

## REFERENCES

1. A. A. Zenin and S. V. Finjakov, "Physics of combustion of energetic binder–nitramine mixtures," in: *Proc. of the* 33*rd Int. Annu. Conf. of ICT*, Fraunhofer Institut Chemische Technologie, Karlsruhe (2002), pp. 6.1–6.14.

2. A. A. Zenin, "Study of combustion mechanism of nitramine–polymer mixture," Report No. R&D 8724-AN-01, European Research Office of the U.S. Army (2000).

3. N. Kubota and T. Sonobe, "Burning rate catalysis of azide/nitramine propellants," in: *Proc. of Twenty-Third Symp.* (*Int.*) *on Combustion*, Combustion Inst., Pittsburgh (1990), pp. 1331–1337.

4. T. A. Litzinger, Y. Lee, and C.-J. Tang, "Experimental studies of nitramine/azide propellant combustion," in: V. Yang, T. B. Brill, and W.-Z. Ren (eds.), *Progress in Astronautics and Aeronautics*, Vol. 185: *Solid Propel-lant Chemistry, Combustion, and Motor Interior Ballistics* (2000), pp. 355–379.

5. E. S. Kim, V. Yang, and Y.-C. Liau, "Modeling of HMX/GAP pseudo-propellant combustion," *Combust. Flame*, **131**, 227–245 (2002).

6. Y.-C. Liau, V. Yang, and S. T. Thynell, "Modeling of RDX/GAP propellant combustion with detailed chemical kinetics," in: V. Yang, T. B. Brill, W.-Z. Ren (eds.), *Progress in Astronautics and Aeronautics*, Vol. 185: *Solid Propellant Chemistry, Combustion, and Motor Interior Ballistics* (2000), pp. 477–500.

7. K. V. Puduppakkam and M. W. Beckstead, "RDX/GAP pseudo-propellant combustion modeling," in: 38*th JAN-NAF Combustion Meeting*, CPIA Publ. No. 712, Vol. I (2002), pp. 143–156.

8. O. P. Korobeinichev, A. A. Paletsky, E. N. Volkov, et al., "Investigation of flame structure of HMX/GAP propellant at 0.5 MPa," in: L. T. DeLuca, L. Galfetti, R. A. Pesce-Rodriguez (eds.), *Novel Energetic Materials and Application*, Proc. of the 9th Int. Workshop Combustion and Propulsion, Grafiche GSS, Bergamo, Italy (2004), Paper 43.

9. A. A. Paletsky, O. P. Korobeinichev, A. G. Tereshchenko, et al., "Flame structure of HMX/GAP propellant at high pressure," *Proc. Combust. Inst.*, **30**, No. 2, 2105–2112 (2005).

10. B. Trusov, *Multi-Purpose ASTRA Software for Modeling Chemical and Phase Equilibria at High Temperatures*, Version 2/24 [in Russian], Bauman Moscow State Technical University (1990).

11. A. Zenin and S. Finjakov, "Physics of combustion of solid mixtures with active binders and new oxidizers," in: *Proc. of the 35th Int. Annu. Conf. of ICT*, Fraunhofer Inst. Chem. Technol., Karlsruhe (2004), pp. 144.1–144.16.

12. O. P. Korobeinichev, L. V. Kuibida, A. A. Paletsky, and A. A. Chernov, "Study of solid propellant flame structure by mass-spectrometric sampling," *Combust. Sci. Technol.*, **113–114**, 557–571 (1996).

13. O. P. Korobeinichev, L. V. Kuibida, E. N. Volkov, and A. G. Shmakov, "Mass spectrometric study of combustion and thermal decomposition of GAP," *Combust. Flame*, **129**, Nos. 1–2, 136–150 (2002).

14. O. P. Korobeinichev, L. V. Kuibida, V. N. Orlov, et al., "Mass-spectrometric sampling of flame structure and chemical reaction kinetics in flames," in: V. L. Tal'roze (ed.), *Mass Spectrometry and Chemical Kinetics* [in Russian], Nauka, Moscow (1985), pp. 73–93.

15. O. P. Korobeinichev, L. V. Kuibida, and V. Zh. Madirbaev, "Chemical structure of HMX flame," *Combust., Expl., Shock Waves*, **20**, No. 3, 282–285 (1984).